Hamiltonian Hopf bifurcation of the hydrogen atom in crossed fields

K. Efstathiou [a,*], R.H. Cushman [b], D.A. Sadovskií [a]

[a] *Université du Littoral, UMR 8101 du CNRS, 59140 Dunkerque, France*
[b] *Mathematisch Instituut, Universiteit Utrecht, 3508 TA Utrecht, The Netherlands*

Abstract

We consider the hydrogen atom in crossed electric and magnetic fields. We prove that near the Stark and Zeeman limits the system goes through two qualitatively different Hamiltonian Hopf bifurcations. We explain in detail the geometry of the bifurcations.
© 2004 Elsevier B.V. All rights reserved.

Keywords: Hamiltonian Hopf bifurcation; Monodromy; Zeeman and Stark limit; Crossed electric and magnetic field

1. Introduction

The hydrogen atom in constant orthogonal electric and magnetic fields is a fundamental atomic system. The system itself and its limiting cases of pure magnetic or electric field (Zeeman and Stark limit, respectively) have been studied to varying degrees of completeness and mathematical sophistication in a series of papers [1–9]. In [10,11] it was shown that as the parameters of the system (the relative field strengths) vary from the Zeeman limit to the Stark limit, there exists an interval of parameter values for which the system has *monodromy*.

It was conjectured there that monodromy is caused by two separate Hamiltonian Hopf bifurcations. The authors of [10] were unable to prove this conjecture because they calculated the relevant normal form (the *second* normal form in the terminology that we use later) only up to terms of second degree. Normalization to higher degree is needed to resolve the degeneracy that appears at the bifurcation.

In this work we prove that the appearance of monodromy as we move away from the Zeeman limit is due to a supercritical Hamiltonian Hopf bifurcation. On the other hand, a subcritical Hamiltonian Hopf bifurcation happens as we leave the monodromy interval and approach the Stark limit. We show that in the latter case the system has monodromy both before and after the bifurcation. The two types of monodromy are qualitatively different, one of

---

* Corresponding author. Tel.: +33-3-28-65-82-63; fax: +33-3-28-65-82-63.
E-mail address: cefstat@purple.univ-littoral.fr (K. Efstathiou).

them being ordinary and the other *non-local monodromy* [12]. The study of these bifurcations is made possible by the computation of the relevant normal form to higher order than was done in [10] and in all other previous work. Notice that due to additional symmetries these bifurcations are highly degenerate. As a result they happen on a microscopic scale: the relevant structures in phase space and the range of parameters in which one can see them are very small. It would be hardly possible to find these bifurcations using a superficial numerical treatment of the problem without powerful analytic techniques, namely normalization (of which there are three different variations in this work) and symmetry reduction.

1.1. Fundamental notions

The hydrogen atom in crossed fields is an example of a perturbed Kepler system. The first step in its study is *Keplerian normalization* which consists of regularization of the singularity of the Kepler potential and normalization of the resulting system [1–7]. In this work we use Kustaanheimo–Stiefel (KS) regularization [13]. The result of KS regularization is a Hamiltonian that is a perturbation of the harmonic oscillator in 1:1:1:1 resonance, with an extra $\mathbf{S}^1$ symmetry due to the flow of the Hamiltonian vector field associated to the KS integral. The normalization of the system with respect to the approximate dynamical $\mathbf{S}^1$ symmetry induced by the unperturbed part of the Hamiltonian can then be easily performed using standard techniques. The consequent reduction in terms of the $\mathbf{T}^2$ oscillator and KS symmetry gives a Poisson system defined on $\mathbf{S}^2 \times \mathbf{S}^2$. The dynamical variables on $\mathbf{S}^2 \times \mathbf{S}^2$ span the $so(4) = so(3) \times so(3)$ algebra.

The important property of the crossed fields system is that after the first normalization the reduced system has yet another approximate $\mathbf{S}^1$ axial symmetry. We perform a second normalization and reduction with respect to this symmetry. The result is an one degree of freedom integrable Poisson system. The second normalization was introduced for perturbed Keplerian problems in [14], see also [15]. It was used for the hydrogen atom in crossed fields in [16–18]. We perform the second normalization to high order using the Lie series algorithm [19,20] for the standard Poisson structure on $so(3) \times so(3)$.

In [10] it was discovered that the hydrogen atom in crossed fields has monodromy for an interval of the parameters. Monodromy was introduced by Duistermaat in [21] as the simplest topological obstruction to the existence of global action-angle variables in integrable Hamiltonian systems. We explain this concept a bit more. Consider a two degree of freedom integrable Hamiltonian system with Hamiltonian function H and second integral J called momentum. Let m_c be an isolated critical value of the energy–momentum map $\mathcal{EM} : \mathbf{R}^4 \to \mathbf{R}^2 : p \mapsto (H(p), J(p))$ and consider a closed path Γ around m_c on the set of regular values of $\mathcal{EM}$. Although for each point $m \in \Gamma$, $\mathcal{EM}^{-1}(m)$ is a $\mathbf{T}^2$ torus, it is not true in general that the $\mathbf{T}^2$ bundle over Γ is trivial, that is, that $\mathcal{EM}^{-1}(\Gamma)$ is diffeomorphic to $\mathbf{S}^1 \times \mathbf{T}^2$. If the bundle over Γ is not trivial we say that the system has monodromy. In [22] it was shown that the system has monodromy if $\mathcal{EM}^{-1}(m_c)$ is a pinched torus.

Monodromy in a parametric family of Hamiltonian systems can appear as the result of a Hamiltonian Hopf bifurcation [23]. This bifurcation is a codimension one bifurcation that happens in Hamiltonian systems with two degrees of freedom. When an equilibrium p of a Hamiltonian H is elliptic–elliptic, then by a theorem of Weinstein [24] there exists a family of periodic orbits emanating from p. When p changes its linear stability type to complex hyperbolic and certain non-degeneracy conditions are satisfied, then two things can happen to this family of periodic orbits. It can either disappear or it can detach from p. In the first case we have a *subcritical* Hamiltonian Hopf bifurcation and in the second a *supercritical* Hamiltonian Hopf bifurcation.

In the case of a supercritical Hamiltonian Hopf bifurcation it is known that the system has monodromy when the equilibrium is complex hyperbolic [23,25]. The reason for this is rather clear. When p is elliptic–elliptic it is connected to a family of periodic orbits that appear as critical points of the energy momentum map $\mathcal{EM}$. Therefore $m_c = \mathcal{EM}(p)$ is not isolated. When p changes linear stability type and becomes complex hyperbolic, the family
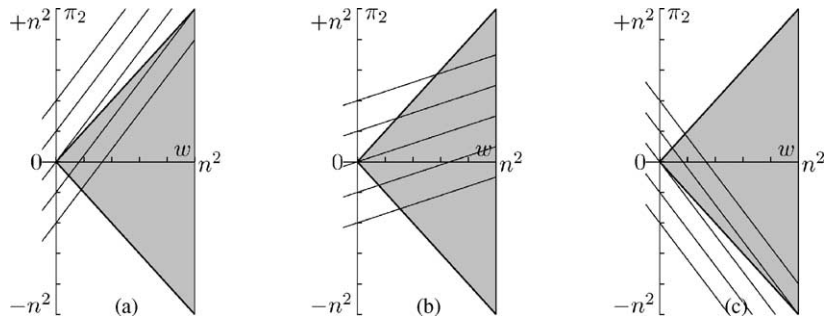
Fig. 1. Relative positions of $V_{n,0}^0$ and the level curves of $\bar{\mathcal{H}}_0$. The shaded region represents $V_{n,0}^0$. (a) Near the Zeeman limit. (b) Monodromy region. (c) Near the Stark limit.

of periodic orbits detaches from p. Therefore in the image of $\mathcal{EM}$, m_c appears as an isolated critical point. Under certain conditions [26] $\mathcal{EM}^{-1}(m_c)$ is a pinched torus and the system has monodromy.

What seems to have gone unnoticed until now is that an integrable Hamiltonian system can have monodromy when it undergoes a subcritical Hamiltonian Hopf bifurcation. We show that this happens in the hydrogen atom in crossed fields.

The second normalization to high degree is a necessary improvement with respect to all previous work, because it lifts the degeneracy when the system goes in and out of the monodromy region. Let us explain the origin of the degeneracy. We denote by n the value of the generator of the oscillator symmetry and by c the value of the generator of the approximate $\mathbf{S}^1$ axial symmetry. For $c = 0$, the fully reduced space $V_{n,0}^0$ in the coordinates (w, π_2) defined in Appendix B.2 is a filled triangle with borders $w = \pm\pi_2$ and $w = n^2$ (see Fig. 1). In [10] only the two-jet of the second normal form $\tilde{\mathcal{H}}$ was computed. To that degree the fully reduced Hamiltonian $\bar{\mathcal{H}}_0$ on $V_{n,0}^0$ is linear in w and π_2. This means that the level sets of $\bar{\mathcal{H}}_0$ are straight lines. The different regimes of the system depend on the relative positions of the level sets of $\bar{\mathcal{H}}_0$ and $V_{n,0}^0$ (Fig. 1). The qualitative changes of the system happen when the level sets of $\bar{\mathcal{H}}_0$ are parallel either to the line $w = \pi_2$ or the line $w = -\pi_2$. Then the reason of the degeneracy is that a small perturbation will curve the level sets of $\bar{\mathcal{H}}_0$ either 'inwards' or 'outwards', see [10]. As we show in Section 4 these cases correspond to qualitatively different Hamiltonian Hopf bifurcations. Therefore in order to lift the degeneracy we need to compute the second normal form $\tilde{\mathcal{H}}$ to a degree such that $\tilde{\mathcal{H}}_c$ is quadratic to w and π_2. We show in Appendix B.2 that because of a discrete symmetry this happens when we compute the four-jet of $\tilde{\mathcal{H}}$, which corresponds to degree 8 in the original KS variables. Following the whole normalization and reduction procedure we find that in turn we have to compute the first normal form up to terms of degree 10.

We now give an outline of the paper. In Section 2 we review the second normalization of the system. In Section 3 we formulate and prove the main result of this paper which is the existence of the two qualitatively different Hamiltonian Hopf bifurcations in the hydrogen atom in crossed fields. Finally, in Section 4 we illustrate and discuss the geometric manifestation of these Hamiltonian Hopf bifurcations in the reduced phase space and explain how monodromy appears near the Zeeman and Stark limits.

2. Review of normalization and reduction

We give a brief review of the Kustaanheimo–Stiefel regularization, the normalization and the reduction of the system following the presentation and notation in [10], where the reader can find more details.

2.1. Hamiltonian

We consider a hydrogen atom with proton at the point 0 in physical space $\mathbf{R}^3$ with variables $Q = (Q_1, Q_2, Q_3)$. The electric field is $\mathbf{E} = (0, F, 0)$ while the magnetic field is $\mathbf{B} = (G, 0, 0)$. The motion of the electron is then described by the Hamiltonian

$$H : \mathbf{R}^6 \to \mathbf{R} : (Q, P) \mapsto H(Q, P) = \frac{1}{2}P^2 - \frac{C}{|Q|} + FQ_2 + \frac{1}{2}G(Q_2P_3 - Q_3P_2) + \frac{1}{8}G^2(Q_2^2 + Q_3^2), \quad (1)$$

where $P = (P_1, P_2, P_3)$ are the conjugate momenta.

In the Hamiltonian H we have ignored all effects due to the spin of the electron and relativistic corrections. In addition we have simplified the two-body problem by considering an infinitely heavy proton.

Instead of F and G we will use the parameters ϵ and a defined in (A.7) of Appendix A.1. The parameter $\epsilon > 0$ represents the total strength of the two fields while a represents the relative strength of the fields and takes values in $[-1, 1]$. When $|a|$ is small the system is near the Stark limit; while when $|a|$ is close to 1 the system is near the Zeeman limit.

2.2. Keplerian normalization

The Keplerian normalization of H (1) consists of the Kustaanheimo–Stiefel regularization followed by normalization and reduction of the resulting system with respect to the $\mathbf{T}^2 = \mathbf{S}^1 \times \mathbf{S}^1$ action generated by the 1:1:1:1 oscillator and KS symmetry. For details see Appendix A.1 or [10]. The final result is a Poisson system defined on the first reduced space $\mathbf{S}^2 \times \mathbf{S}^2$, which can be described by coordinate functions $x = (x_1, x_2, x_3)$ and $y = (y_1, y_2, y_3)$ that satisfy the conditions

$$x_1^2 + x_2^2 + x_3^2 = \tfrac{1}{4}n^2, \qquad y_1^2 + y_2^2 + y_3^2 = \tfrac{1}{4}n^2. \tag{2}$$

Here n is the value of the generator of the oscillator symmetry. The dynamical variables x, y span the algebra so(3) $\times$ so(3) = so(4). Specifically, the Poisson structure on $\mathbf{S}^2 \times \mathbf{S}^2$ is

$$\{x_i, x_j\} = \sum_k \varepsilon_{ijk} x_k, \qquad \{y_i, y_j\} = \sum_k \varepsilon_{ijk} y_k, \qquad \{x_i, y_j\} = 0. \tag{3}$$

The first reduced Hamiltonian defined on $\mathbf{S}^2 \times \mathbf{S}^2$ can be written in terms of (x, y, n) variables as

$$\mathcal{H} = \mathcal{H}_1 + \epsilon \mathcal{H}_2 + \epsilon^2 \mathcal{H}_3 + \epsilon^3 \mathcal{H}_4. \tag{4}$$

The lowest order non-trivial term is

$$\mathcal{H}_1 = x_1 + y_1. \tag{5}$$

Each $\mathcal{H}_j$ is a homogeneous polynomial of degree j in (x, y, n). For $j \geq 2$ the terms $\mathcal{H}_j$ can be computed in a straightforward way from Table 2 using the relations (A.17) and (A.18).

2.3. Second normalization

$\mathcal{H}_1$ generates an $\mathbf{S}^1$ action Φ on $\mathbf{S}^2 \times \mathbf{S}^2$ given by

$$\Phi : \mathbf{S}^1 \times (\mathbf{S}^2 \times \mathbf{S}^2) \to (\mathbf{S}^2 \times \mathbf{S}^2) : (t, (x, y)) \to (x_1, R(t)(x_2, x_3)^{\mathrm{T}}, y_1, R(t)(y_2, y_3)^{\mathrm{T}}), \tag{6}$$

where

$$R(t) = \begin{pmatrix} \cos t & -\sin t \\ \sin t & \cos t \end{pmatrix}.$$

We normalize the Hamiltonian $\mathcal{H}$ (4) with respect to the action Φ. First define new variables

$$z_1 = \frac{1}{2}x_1, \qquad z_2 = \frac{1}{2\sqrt{2}}(x_2 + \mathrm{i}x_3), \qquad \bar{z}_2 = \frac{1}{2\sqrt{2}}(x_2 - \mathrm{i}x_3),$$

$$w_1 = \frac{1}{2}y_1, \qquad w_2 = \frac{1}{2\sqrt{2}}(y_2 + \mathrm{i}y_3), \qquad \bar{w}_3 = \frac{1}{2\sqrt{2}}(y_2 - \mathrm{i}y_3). \tag{7}$$

Then notice that

$$\{z_1, z_2\} = \frac{z_2}{2\mathrm{i}}, \qquad \{z_1, \bar{z}_2\} = -\frac{\bar{z}_2}{2\mathrm{i}}, \qquad \{z_2, \bar{z}_2\} = \frac{z_1}{2\mathrm{i}}. \tag{8}$$

In these variables $\mathcal{H}_1$ becomes $\mathcal{H}_1 = 2(z_1 + w_1)$ and the action of $\mathrm{ad}_{\mathcal{H}_1} = \{\mathcal{H}_1, \cdot\}$ on a monomial $z^a w^b = z_1^{a_1} z_2^{a_2} \bar{z}_2^{a_3} w_1^{b_1} w_2^{b_2} \bar{w}_2^{b_3}$ is diagonal:

$$\{\mathcal{H}_1, z^a w^b\} = -\mathrm{i}(a_2 - a_3 + b_2 - b_3)z^a w^b. \tag{9}$$

Therefore the variables z and w are particularly suitable for the application of the standard Lie series algorithm [19,20] for the computation of the second normal form, since they trivialize the task of solving the homological equation.

Remark 1. Another way to perform the second normalization is to express $\mathcal{H}$ (4) in terms of the original variables (q, p). Then normalization can be performed in these variables and the result can be re-expressed in terms of the variables (x, y).

The result of second normalization is the Hamiltonian

$$\tilde{\mathcal{H}} = \tilde{\mathcal{H}}_1 + \epsilon\tilde{\mathcal{H}}_2 + \epsilon^2\tilde{\mathcal{H}}_3 + \epsilon^3\tilde{\mathcal{H}}_4, \tag{10}$$

where each term $\tilde{\mathcal{H}}_j$ is a homogeneous polynomial of degree j in (x, y, n). Explicit expressions for $\tilde{\mathcal{H}}$ can be easily obtained from the expressions for the second reduced Hamiltonian $\hat{\mathcal{H}}$ given in Table 3.

The points $p_\pm = (n/2)(\pm 1, 0, 0, \mp 1, 0, 0)$ and $z_\pm = (n/2)(\pm 1, 0, 0, \pm 1, 0, 0)$ are fixed points of the $\mathbf{S}^1$ action Φ. Therefore [27] they are equilibria of any Φ invariant Hamiltonian on $\mathbf{S}^2 \times \mathbf{S}^2$. In particular, they are equilibria of $\tilde{\mathcal{H}}$ (10).

3. The Hamiltonian Hopf bifurcations

In this section we prove the following theorem which is the main result of the paper.

Theorem 1. *The equilibria* $p_\pm = (n/2)(\pm 1, 0, 0, \mp 1, 0, 0)$ *of the second normalized Hamiltonian* $\tilde{\mathcal{H}}$ *(10) on* $\mathbf{S}^2 \times \mathbf{S}^2$ *undergo a supercritical Hamiltonian Hopf bifurcation at* $a = a_1(n\epsilon)$ *and a subcritical Hamiltonian Hopf bifurcation at* $a = a_2(n\epsilon)$. *Here* a_1 *and* a_2 *are functions of* $\delta = n\epsilon$ *given in* (33) *and* (34).

Sketch of the proof. The first step of the proof is to find a local chart (Q, P) on $\mathbf{S}^2 \times \mathbf{S}^2$ near the point p_+. The symplectic form in the chart (Q, P) is in Darboux form only up to constant terms:

$$\omega = \mathrm{d}Q_1 \wedge \mathrm{d}P_1 + \mathrm{d}Q_2 \wedge \mathrm{d}P_2 + \omega_2(Q, P) + \omega_4(Q, P) + \cdots \tag{11}$$

because we are working on the curved space $\mathbf{S}^2 \times \mathbf{S}^2$. Here ω_2 and ω_4 are two-forms of degrees 2 and 4, respectively. In order to study the local dynamics near the equilibrium point p_+ we need to *flatten* the symplectic form to Darboux form at an appropriate order, using a constructive version of the Darboux theorem [28]. The result of flattening is a chart (q, p) in which the symplectic form is

$$\omega = \mathrm{d}q_1 \wedge \mathrm{d}p_1 + \mathrm{d}q_2 \wedge \mathrm{d}p_2 + \tilde{\omega}_4(q, p) + \cdots . \tag{12}$$

After flattening the symplectic form and expressing the local Hamiltonian in the chart (q, p), we reduce the local Hamiltonian with respect to the $\mathbf{S}^1$ symmetry that is induced on the local chart from the Φ action (6) on $\mathbf{S}^2 \times \mathbf{S}^2$. The multiplicative ring of invariants of the induced $\mathbf{S}^1$ symmetry is generated by the quadratic polynomials M, N, T and S in the variables (q, p). S is the generator of the $\mathbf{S}^1$ symmetry and M, N generate nilpotent linear Hamiltonian vector fields.

We denote by G the reduced local Hamiltonian and by G_j the j-degree part of G, where the degree is defined in terms of the variables q and p. The next step is to bring G_2 into versal normal form for the Hamiltonian Hopf bifurcation, namely

$$G_2 = \alpha M + N + \Omega S, \tag{13}$$

or

$$G_2 = M + \beta N + \Omega S. \tag{14}$$

We also have to check that certain transversality conditions are satisfied when $\alpha = 0$ or $\beta = 0$. This proves that the local Hamiltonian G goes through a *linear* Hamiltonian Hopf bifurcation.

The final step is to normalize G with respect to M (or N). If, after the normalization, the coefficient of M^2 (or N^2) is zero, then the bifurcation is degenerate. If the coefficient is positive the bifurcation is *supercritical* and if it is negative the bifurcation is *subcritical*.

Remark 2. In order to study the Hamiltonian Hopf bifurcation we need at least the four-jet of G. Recall that in order to lift the degeneracy discussed in Section 1 and in Appendix B.2 we need to consider the four-jet of $\tilde{\mathcal{H}}$. If we make the computations that lead to the proof of Theorem 1 using the three-jet of $\tilde{\mathcal{H}}$ (instead of its four-jet) we find that the coefficient of M^2 (or N^2) is zero. This is how the degeneracy manifests itself in the local analysis of this section.

Remark 3. The hydrogen atom in crossed fields problem has two parameters $\delta = n\epsilon$ and a. In the formulation of Theorem 1 we treat the family $\tilde{\mathcal{H}}$ as a one-parameter family keeping δ constant and small and varying only a. Despite this, we can consider more general one-parameter subfamilies of $\tilde{H}$ under certain transversality conditions in parameter space on which we elaborate in the following sections.

In the following sections we fill in the details of the argument sketched above.

3.1. Local chart

We define a local chart on $\mathbf{S}^2 \times \mathbf{S}^2$ near the point p_+ with coordinates Q_1, Q_2, P_1, P_2 given by

$$\begin{aligned} x_1 &= (\tfrac{1}{4}n^2 - \tfrac{1}{2}nQ_1^2 - \tfrac{1}{2}nP_1^2)^{1/2}, & x_2 &= (\tfrac{1}{2}n)^{1/2}Q_1, & x_3 &= (\tfrac{1}{2}n)^{1/2}P_1, \\ y_1 &= -(\tfrac{1}{4}n^2 - \tfrac{1}{2}nQ_2^2 - \tfrac{1}{2}nP_2^2)^{1/2}, & y_2 &= (\tfrac{1}{2}n)^{1/2}P_2, & y_3 &= (\tfrac{1}{2}n)^{1/2}Q_2. \end{aligned}$$

Note that the coordinate functions Q and P are not canonically conjugate since the symplectic two-form in these coordinates is

$$\omega = \mathrm{d}Q_1 \wedge \mathrm{d}P_1 + \mathrm{d}Q_2 \wedge \mathrm{d}P_2 + \text{(higher order terms)}. \tag{15}$$

We first make the transformation

$$Q_1 = -\tfrac{1}{2}(p_1 + p_2 + q_1 - q_2), \qquad Q_2 = -\tfrac{1}{2}(p_1 - p_2 + q_1 + q_2),$$
$$P_1 = \tfrac{1}{2}(-p_1 + p_2 + q_1 + q_2), \qquad P_2 = -\tfrac{1}{2}(p_1 + p_2 - q_1 + q_2).$$

The coordinate functions q and p are not canonical either and the symplectic two-form has the form

$$\omega = \omega_0 + \omega_2 + \omega_4 + \cdots, \tag{16}$$

where

$$\omega_0 = \mathrm{d}q_1 \wedge \mathrm{d}p_1 + \mathrm{d}q_2 \wedge \mathrm{d}p_2, \tag{17}$$

and

$$\omega_2 = \frac{1}{2n}(p_1^2 + p_2^2 + q_1^2 + q_2^2)(\mathrm{d}q_1 \wedge \mathrm{d}p_1 + \mathrm{d}q_2 \wedge \mathrm{d}p_2) + \frac{1}{n}(p_1 q_2 - p_2 q_1)(\mathrm{d}q_1 \wedge \mathrm{d}q_2 + \mathrm{d}p_1 \wedge \mathrm{d}p_2). \tag{18}$$

3.2. Flattening of the symplectic form

The first step in order to study the local behavior of the Hamiltonian system near p_+ is to *flatten* the symplectic form ω (16) up to second degree terms. In other words, we need to eliminate the term ω_2. This means that we find a near identity transformation ϕ such that

$$\phi^* \omega = \omega_0 + \tilde{\omega}_4 + \cdots, \tag{19}$$

where the components of $\tilde{\omega}_4$ are homogeneous polynomials of degree 4.

The following lemma explains why flattening ω up to fourth degree terms is sufficient.

Lemma 1. *Consider a Hamiltonian $H = H_2 + H_3 + \cdots$ and a symplectic form $\omega = \omega_0 + \omega_j + \cdots$, i.e. $\omega_k = 0$ for $1 \le k \le j - 1$. Then the j-jet of the Hamiltonian vector field X of H with respect to ω is equal to the j-jet of the Hamiltonian vector field Y of H with respect to ω_0.*

Proof. Write the Hamiltonian vector field X as

$$X = X_1 + X_2 + X_3 + \cdots, \tag{20}$$

where the components of X_j are homogeneous polynomials of degree j in (q, p). X is the solution of the equation $X \lrcorner \omega = \mathrm{d}H$, or

$$(X_1 + X_2 + X_3 + \cdots) \lrcorner (\omega_0 + \omega_j + \cdots) = \mathrm{d}H_2 + \mathrm{d}H_3 + \cdots. \tag{21}$$

Splitting this equation into terms of equal degree we get

$$X_k \lrcorner \omega_0 = \mathrm{d}H_{1+k}, \quad 1 \le k \le j, \qquad X_k \lrcorner \omega_0 + \sum_{l=1}^{k-j} X_l \lrcorner \omega_{j+1-l} = \mathrm{d}H_{1+k}, \quad k \ge j+1$$

from which the lemma follows. $\square$

Applying Lemma 1 to the case at hand shows that when the first non-zero terms of the symplectic form after ω_0 are of degree 4 then we can study Hamiltonians of degree up to 5 without any more flattening.

Flattening of the symplectic form is done using the method described in [28]. Specifically we find a vector field X such that $\mathcal{L}_X \omega_0 + \omega_2 = 0$. An X satisfying

$$X \lrcorner \omega_0 = -\frac{1}{4} \left(q_1 \frac{\partial}{\partial q_1} + q_2 \frac{\partial}{\partial q_2} + p_1 \frac{\partial}{\partial p_1} + p_2 \frac{\partial}{\partial p_2} \right) \lrcorner \omega_2 \tag{22}$$

does the job. A short computation gives

$$\begin{aligned}
X = \frac{1}{8n} \Bigg(& (-q_1(q_1^2 + q_2^2 + p_1^2 + p_2^2) - 2p_2(p_2 q_1 - p_1 q_2)) \frac{\partial}{\partial q_1} + (-q_2(q_1^2 + q_2^2 + p_1^2 + p_2^2) \\
& + 2p_1(p_2 q_1 - p_1 q_2)) \frac{\partial}{\partial q_2} + (-p_1(q_1^2 + q_2^2 + p_1^2 + p_2^2) + 2q_2(p_2 q_1 - p_1 q_2)) \frac{\partial}{\partial p_1} \\
& + (-p_2(q_1^2 + q_2^2 + p_1^2 + p_2^2) - 2q_1(p_2 q_1 - p_1 q_2)) \frac{\partial}{\partial p_2} \Bigg).
\end{aligned} \tag{23}$$

Let $\mathcal{H}^{\text{loc}}$ be the Taylor expansion of $\tilde{\mathcal{H}}$ (10), expressed in coordinates (q, p) near $(0, 0)$. A short computation shows that $\mathcal{H}^{\text{loc}}$ has the form

$$\mathcal{H}^{\text{loc}} = \mathcal{H}_2^{\text{loc}} + \mathcal{H}_4^{\text{loc}} + \cdots, \tag{24}$$

where each $\mathcal{H}_j^{\text{loc}}$ is a homogeneous polynomial of degree j in (q, p). The final step is to use the transformation ϕ generated by the flow of the vector field X in order to obtain the Hamiltonian $\phi^* \mathcal{H}^{\text{loc}}$ in coordinates in which ω has been flattened to terms of degree 2. We have

$$\phi^* \mathcal{H}^{\text{loc}} = \mathcal{H}_2^{\text{loc}} + (\mathcal{L}_X \mathcal{H}_2^{\text{loc}} + \mathcal{H}_4^{\text{loc}}) + \cdots, \tag{25}$$

where $\mathcal{H}_j^{\text{loc}}$ is the degree j term of $\mathcal{H}^{\text{loc}}$.

3.3. $\mathbf{S}^1$ symmetry

The Hamiltonian $\mathcal{H}_1$ (5) generates a Hamiltonian $\mathbf{S}^1$ action Φ on $\mathbf{S}^2 \times \mathbf{S}^2$ that induces an $\mathbf{S}^1$ action on the local chart. A computation shows that the action induced on the chart (q, p) is

$$\tilde{\Phi} : \mathbf{S}^1 \times \mathbf{R}^4 \to \mathbf{R}^4 : (t, (q, p)) \mapsto (R(t)q, R(t)p), \tag{26}$$

where

$$R(t) = \begin{pmatrix} \cos t & -\sin t \\ \sin t & \cos t \end{pmatrix}.$$

Lemma 2. *The algebra* $\mathbf{R}[q, p]^{\tilde{\Phi}}$ *of* $\tilde{\Phi}$*-invariant polynomials is generated by*

$$M = \tfrac{1}{2}(p_1^2 + p_2^2), \qquad N = \tfrac{1}{2}(q_1^2 + q_2^2), \qquad S = q_1 p_2 - q_2 p_1, \qquad T = q_1 p_1 + q_2 p_2, \tag{27}$$

which satisfy the relation

$$S^2 + T^2 = 4MN, \quad M \geq 0, \ N \geq 0. \tag{28}$$

Note that S is the generator of $\tilde{\Phi}$.

Table 1
Coefficients of $G = G_2 + \epsilon G_4$

Coefficients of terms of $1728G_2$	
M	$-432\delta + 864a^4\delta - 591\delta^3 + 1194a^2\delta^3 - 480a^4\delta^3 - 84a^6\delta^3 + 66a^8\delta^3 - 588a^{10}\delta^3 + 492a^{12}\delta^3$
N	$-432\delta + 1728a^2\delta + 864a^4\delta - 591\delta^3 + 3078a^2\delta^3 - 3480a^4\delta^3 - 380a^6\delta^3 - 94a^8\delta^3 - 204a^{10}\delta^3 + 492a^{12}\delta^3$
S	$-1728 - 984\delta^2 + 2448a^2\delta^2 - 1008a^4\delta^2 - 960a^6\delta^2 + 504a^8\delta^2$

Coefficients of terms of $3456G_4$	
NS	$-2064\delta + 7296a^2\delta - 624a^4\delta + 4320a^6\delta - 2448a^8\delta$
MS	$-2064\delta + 768a^2\delta + 144a^4\delta + 4896a^6\delta - 2448a^8\delta$
MN	$-864 + 1728a^2 + 1728a^4 - 576\delta^2 + 1768a^2\delta^2 - 5392a^4\delta^2 - 2360a^6\delta^2 + 7844a^8\delta^2 - 4080a^{10}\delta^2 + 3984a^{12}\delta^2$
M^2	$432 - 864a^4 + 288\delta^2 - 1082a^2\delta^2 + 1260a^4\delta^2 + 2540a^6\delta^2 - 3978a^8\delta^2 + 2604a^{10}\delta^2 - 1992a^{12}\delta^2$
N^2	$432 - 1728a^2 - 864a^4 + 288\delta^2 - 686a^2\delta^2 + 52a^4\delta^2 + 12a^6\delta^2 - 3290a^8\delta^2 + 900a^{10}\delta^2 - 1992a^{12}\delta^2$
S^2	$-2016 + 1152a^2 - 1728a^4 - 6392\delta^2 + 17\,048a^2\delta^2 - 9000a^4\delta^2 + 616a^6\delta^2 - 6628a^8\delta^2 + 8304a^{10}\delta^2 - 3984a^{12}\delta^2$

Here $\delta = n\epsilon$ and a is defined in (A.7).

The Poisson structure on $\mathbf{R}^4$ is

$$\{M, N\} = -T, \qquad \{M, T\} = -2M, \qquad \{N, T\} = 2N, \tag{29}$$

and $\{M, S\} = \{N, S\} = \{T, S\} = 0$.

Because of Lemma 2 the Hamiltonian $\mathcal{H}^{\mathrm{loc}}$ can be expressed in terms of the invariants (27). Moreover since the flattening transformation ϕ preserves the $\mathbf{S}^1$ symmetry the same applies to the 'flattened' local Hamiltonian $\phi^*\mathcal{H}^{\mathrm{loc}}$.

Therefore truncation of the local Hamiltonian to terms of degree 4, flattening and expression in terms of the invariants (27) gives the Hamiltonian

$$G = G_2 + \epsilon G_4. \tag{30}$$

Here G_2 and G_4 are homogeneous polynomials of the invariant polynomials (27) of degrees 1 and 2, respectively. Explicit expressions of G_2 and G_4 are given in Table 1.

3.4. Linear Hamiltonian Hopf bifurcation

The reduced local Hamiltonian G (30) is given in Table 1. We write the linear part of this Hamiltonian as

$$G_2 = \delta A(a, \delta)M + \delta B(a, \delta)N + C(a, \delta)S, \tag{31}$$

where $\delta = n\epsilon$ and the coefficients $A(a, \delta)$, $B(a, \delta)$ and $C(a, \delta)$ can be read off the first entries in Table 1. Since G depends on the parameters a and $\delta = n\epsilon$ we also write $G_{a,\delta}$ instead of G.

The eigenvalues of the Hamiltonian matrix of G_2 are

$$\pm\mathrm{i}(C \pm \delta\sqrt{AB}). \tag{32}$$

It is obvious from (32) that the origin changes linear stability type when one of A or B changes sign. Specifically, when $AB < 0$ the origin is complex hyperbolic; while when $AB > 0$ it is elliptic–elliptic. At $A = 0$ or $B = 0$ the eigenvalues are $(\mathrm{i}C, \mathrm{i}C, -\mathrm{i}C, -\mathrm{i}C)$ but the Hamiltonian matrix of G_2 is not semisimple (Fig. 2).

Let $\mathcal{W}_A$ and $\mathcal{W}_B$ be the curves on the parameter plane (a, δ) on which $A(a, \delta) = 0$ and $B(a, \delta) = 0$, respectively. Let $a_1(\delta)$ be the function that satisfies $A(a_1(\delta), \delta) = 0$ and $a_2(\delta)$ the function that satisfies $B(a_2(\delta), \delta) = 0$. For small δ, the Taylor series of the squares of these two functions are

$$a_1(\delta)^2 = \frac{1}{\sqrt{2}} + \frac{-335 + 251\sqrt{2}}{576}\delta^2 + \mathrm{O}(\delta^4), \tag{33}$$
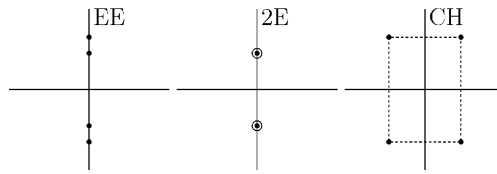
Fig. 2. The movement of eigenvalues at a linear Hamiltonian Hopf bifurcation. EE: elliptic–elliptic, 2E: degenerate elliptic, CH: complex hyperbolic.

and

$$a_2(\delta)^2 = \frac{\sqrt{6} - 2}{2} + \frac{58\,875 - 23\,596\sqrt{6}}{5184}\delta^2 + \mathrm{O}(\delta^4). \tag{34}$$

The curves $\mathcal{W}_A$ and $\mathcal{W}_B$ are depicted in Fig. 3. We note that they do not intersect.

We prove the following lemma.

Lemma 3. *The one-parameter family of quadratic Hamiltonians $s \mapsto G_{a(s),\delta(s)}$ goes through a linear Hamiltonian Hopf bifurcation when the curve $\mathcal{C} : s \mapsto (a(s), \delta(s))$ crosses one of the curves $\mathcal{W}_A$ or $\mathcal{W}_B$ transversely at a point with $\delta > 0$.*

Proof. Consider first the case in which $\mathcal{C}$ crosses $\mathcal{W}_A$ transversely. This means that there is an s_1 such that $A(a(s_1), \delta(s_1)) = 0$ and $\delta(s_1) > 0$. Since $\mathcal{W}_A$ and $\mathcal{W}_B$ do not intersect, we can find a neighborhood U of s_1 such that for all $s \in U$ $B(a(s), \delta(s)) \neq 0$.

We rescale G (30) by dividing by $\delta B(a, \delta)$. Let

$$\tilde{G} = \tilde{G}_2 + \epsilon \tilde{G}_4 = \frac{G}{\delta B(a, \delta)}. \tag{35}$$

The quadratic part of $\tilde{G}$ is

$$\tilde{G}_2 = \alpha(a, \delta)M + N + \Omega_1(a, \delta)S, \tag{36}$$

where $\alpha(a, \delta) = A(a, \delta)/B(a, \delta)$ and $\Omega_1(a, \delta) = C(a, \delta)/(\delta B(a, \delta))$. Clearly $\alpha(a(s_1), \delta(s_1)) = 0$.
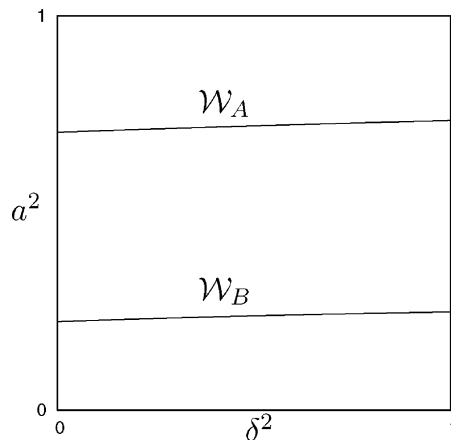

Fig. 3. Bifurcation sets. In the proof we consider curves $s \mapsto (a(s), \delta(s))$ in parameter space for which $\delta = n\epsilon$ is small and which intersect $\mathcal{W}_A$ and $\mathcal{W}_B$ transversely.

The Hamiltonian matrix of $\tilde{G}_2$ is

$$
Y_1(a, \delta) = \begin{pmatrix} 0 & -\Omega_1(a, \delta) & 1 & 0 \\ \Omega_1(a, \delta) & 0 & 0 & 1 \\ -\alpha(a, \delta) & 0 & 0 & -\Omega_1(a, \delta) \\ 0 & -\alpha(a, \delta) & \Omega_1(a, \delta) & 0 \end{pmatrix}. \tag{37}
$$

The one-parameter family of infinitesimally symplectic matrices $s \mapsto \tilde{Y}_1(s) = Y_1(a(s), \delta(s))$ is in normal form for s near s_1. Note that

$$
\tilde{Y}_1(s_1) = \begin{pmatrix} 0 & -\Omega_1^0 & 1 & 0 \\ \Omega_1^0 & 0 & 0 & 1 \\ 0 & 0 & 0 & -\Omega_1^0 \\ 0 & 0 & \Omega_1^0 & 0 \end{pmatrix}, \tag{38}
$$

where $\Omega_1^0 = \Omega_1(a(s_1), \delta(s_1))$. A straightforward computation shows that $\Omega_1^0 \neq 0$. Because $\mathcal{C}$ intersects $\mathcal{W}_A$ transversely we have that

$$
\frac{\mathrm{d}\alpha(a(s), \delta(s))}{\mathrm{d}s}\bigg|_{s=s_1} \neq 0. \tag{39}
$$

Therefore the curve $s \mapsto \tilde{G}_2(s)$ undergoes a linear Hamiltonian Hopf bifurcation at s_1.

The treatment of the second case is almost identical. In this case let s_2 be such that $B(a(s_2), \delta(s_2)) = 0$. We can find a neighborhood U of s_2 such that for all $s \in U$ $A(a(s), \delta(s)) \neq 0$. We rescale G dividing by $\delta A(a, \delta)$. Let

$$
\hat{G} = \hat{G}_2 + \epsilon \hat{G}_4 = \frac{G}{\delta A(a, \delta)}. \tag{40}
$$

The quadratic part of $\hat{G}$ becomes

$$
\hat{G}_2 = M + \beta(a, \delta)N + \Omega_2(a, \delta)S, \tag{41}
$$

where $\beta(a, \delta) = B(a, \delta)/A(a, \delta)$ and $\Omega_2(a, \delta) = C(a, \delta)/(\delta A(a, \delta))$. Clearly $\beta(a(s_2), \delta(s_2)) = 0$.

The Hamiltonian matrix of $\hat{G}_2$ is

$$
Y_2(a, \delta) = \begin{pmatrix} 0 & -\Omega_2(a, \delta) & \beta(a, \delta) & 0 \\ \Omega_2(a, \delta) & 0 & 0 & \beta(a, \delta) \\ -1 & 0 & 0 & -\Omega_2(a, \delta) \\ 0 & -1 & \Omega_2(a, \delta) & 0 \end{pmatrix}. \tag{42}
$$

The one-parameter family of infinitesimally symplectic matrices $s \mapsto \tilde{Y}_2(s) = Y_2(a(s), \delta(s))$ is already in normal form near s_2. Notice that

$$
\tilde{Y}_2(s_0) = \begin{pmatrix} 0 & -\Omega_2^0 & 0 & 0 \\ \Omega_2^0 & 0 & 0 & 0 \\ -1 & 0 & 0 & -\Omega_2^0 \\ 0 & -1 & \Omega_2^0 & 0 \end{pmatrix}, \tag{43}
$$

where $\Omega_2^0 = \Omega_2(a(s_2), \delta(s_2))$. A straightforward computation shows that $\Omega_2^0 \neq 0$. Moreover because $\mathcal{C}$ intersects $\mathcal{W}_B$ transversally we have that

$$
\frac{\mathrm{d}\beta(a(s), \delta(s))}{\mathrm{d}s}\bigg|_{s=s_2} \neq 0. \tag{44}
$$

Therefore the family $s \mapsto \hat{G}_2(s)$ undergoes a linear Hamiltonian Hopf bifurcation at s_2. $\qquad\square$

3.5. Nonlinear Hamiltonian Hopf bifurcation

In this section we prove the following lemma.

Lemma 4. *Any one-parameter family $s \mapsto G_{a(s),\delta(s)}$ that crosses the curve $\mathcal{W}_A$ transversely at a point with $\delta > 0$ goes through a supercritical Hamiltonian Hopf bifurcation.*

Proof. We begin with the rescaled Hamiltonian $\tilde{G}$ (35) with

$$\tilde{G}_2 = \alpha(a, \delta)M + N + \Omega(a, \delta)S \tag{45}$$

from Lemma 3. We have already proved that $s \mapsto \tilde{G}_2(s)$ goes through a linear Hamiltonian Hopf bifurcation at s_1.

We normalize the Hamiltonian $\tilde{G}$ (35) with respect to N using the generator

$$W = c_1 NT + c_2 ST + c_3 MT. \tag{46}$$

The coefficients c_i are determined by demanding that only the terms M^2, S^2 and MS appear in the quadratic part of the normal form. Specifically, we have

$$\exp(\epsilon \mathcal{L}_W)\tilde{G} = (1 + \epsilon \, \mathrm{ad}_W + \mathrm{O}(\epsilon^2))(\tilde{G}_2 + \epsilon \tilde{G}_4 + \mathrm{O}(\epsilon^2)) = \tilde{G}_2 + \epsilon(\tilde{G}_4 + \{W, \tilde{G}_2\}) + \mathrm{O}(\epsilon^2)$$
$$= \tilde{G}_2 + \tilde{\mathcal{G}}_4 + \mathrm{O}(\epsilon^2). \tag{47}$$

The term $\{W, \tilde{G}_2\}$ is equal to

$$\{W, \tilde{G}_2\} = (6c_1\alpha - 6c_3)MN + (c_3 - c_1\alpha)S^2 - 2c_1 N^2 + 2c_3 \alpha M^2 + 2c_2 \alpha MS - 2c_2 NS. \tag{48}$$

At the bifurcation $\alpha = 0$. Therefore

$$\{W, \tilde{G}_2\} = -6c_3 MN + c_3 S^2 - 2c_1 N^2 - 2c_2 NS. \tag{49}$$

By choosing c_1, c_2 and c_3 appropriately it is clear that we can ensure that $\tilde{\mathcal{G}}_4$ (47) is free of terms MN, N^2 and NS.

At $a = a_1(\delta)$ (33) we have

$$\tilde{\mathcal{G}}_4 = M^2(0.0922\delta + 0.0124742\delta^3) + MS(-0.135 + 0.0484\delta^2) + S^2\left(-0.678\frac{1}{\delta} + 0.03\delta - 0.00671\delta^3\right) \tag{50}$$

(the numbers given are approximate). Since the coefficient of M^2 is positive (for $\delta > 0$) the lemma follows. $\quad\square$

Lemma 5. *Any one-parameter family $s \mapsto G_{a(s),\delta(s)}$ that crosses transversaly the line $\mathcal{W}_B$ at a point with $\delta > 0$ goes through a subcritical Hamiltonian Hopf bifurcation.*

Proof. Again we begin with the rescaled Hamiltonian $\hat{G}$ (40) with

$$\hat{G}_2 = M + \beta(a, \delta)N + \Omega(a, \delta)S. \tag{51}$$

We normalize $\hat{G}$ (40) with respect to M using the generator

$$W = c_1 NT + c_2 ST + c_3 MT, \tag{52}$$

where the coefficients c_i in this case are determined by demanding that in the quadratic part $\hat{\mathcal{G}}_4$ of the normal form appear only terms N^2, S^2 and NS. We find

$$\hat{\mathcal{G}}_4 = N^2(-0.0628\delta + 0.118\delta^3) + NS(0.531 - 0.822\delta^2) + S^2\left(2.541\frac{1}{\delta} + 1.846\delta - 1.950\delta^3\right) + \mathrm{O}(\delta^4). \tag{53}$$

In this case the coefficient of N^2 is negative for small δ and we have a subcritical Hamiltonian Hopf bifurcation. $\quad\square$

4. Geometric analysis of the Hamiltonian Hopf bifurcation on the fully reduced space

The original Hamiltonian (1) is invariant with respect to the $\mathbf{Z}_2 \times \mathbf{Z}_2$ action detailed in Appendix B.2. Therefore the Hamiltonian $\tilde{\mathcal{H}}$ (10) is invariant with respect to the induced $\mathbf{Z}_2 \times \mathbf{Z}_2$ action on $\mathbf{S}^2 \times \mathbf{S}^2$. Reduction of $\tilde{\mathcal{H}}$ with respect to the $\mathbf{S}^1$ action Φ (6) and the discrete symmetry $\mathbf{Z}_2 \times \mathbf{Z}_2$ gives the fully reduced Hamiltonian $\bar{\mathcal{H}}_c$ on the fully reduced space $V_{n,c}^0$ with coordinates (w, π_2). Details for this reduction are given in Appendix B.2. Here c is the value of $\mathcal{H}_1$ (5) which is the generator of Φ. In the fully reduced space $V_{n,0}^0$, the point $p = (0, 0)$ corresponds to the points $p_\pm$ that undergo the Hamiltonian Hopf bifurcation studied in Section 3.

Stationary points of $\bar{\mathcal{H}}_c$ correspond to periodic orbits of $\tilde{\mathcal{H}}$ (10) on $\mathbf{S}^2 \times \mathbf{S}^2$. In turn they correspond to periodic orbits of $\mathcal{H}$ (4) in the range of validity of the first normal form. The equilibria of the fully reduced Hamiltonian vector field $X_{\bar{\mathcal{H}}_c}$ are the points of tangency between the level curves of $\bar{\mathcal{H}}_c$ and $V_{n,c}^*$.

When the level curves of $\bar{\mathcal{H}}_0$ become tangent to $V_{n,0}^*$ (i.e. to one of the lines $w = \pm\pi_2$) the system goes through a Hamiltonian Hopf bifurcation. The exact type of the bifurcation depends on how the level curves of $\bar{\mathcal{H}}_0$ are curved with respect to $V_{n,0}^*$. We distinguish two cases, see Fig. 4.

In the first case (Figs. 4a and b) the level curves of $\bar{\mathcal{H}}_0$ 'bend outwards', that is, when the level curve that passes through p becomes tangent to the line $w = \pi_2$ the rest of the level curve stays outside $V_{n,0}^0$. As the parameters of the Hamiltonian change, the slope of the level curves also changes. Note here that the shape of the curves also changes slightly. In order to understand qualitatively what happens, it is enough to consider only the change of slope. Consider the level curve of $\bar{\mathcal{H}}_0$ that passes through p and let $w = f(\pi_2)$ be defined so that $\bar{\mathcal{H}}_0(f(\pi_2), \pi_2) = 0$ near $\pi_2 = 0$. We denote $\lambda = f'(0)$, i.e. λ is the slope at p of the level curve of $\bar{\mathcal{H}}_0$ that passes through p.

When $\lambda > 1$ (Fig. 4a) there are tangencies between the level curves of $\bar{\mathcal{H}}_c$ and $V_{n,c}^*$ for c close to 0. This means that there are equilibria of $\bar{\mathcal{H}}_c$ arbitrarily close to p and therefore periodic orbits of $\tilde{\mathcal{H}}$ attach to p_+. When $\lambda < 1$ (Fig. 4b) the level curves that pass near p enter $V_{n,0}^0$ in such a way that they intersect transversely all $V_{n,c}^*$ with c close to 0, and only for c greater than some value c_0 do they become tangent to $V_{n,c}^*$. This means that there are no critical points of $\bar{\mathcal{H}}_c$ near p, but there do exist such critical points further away. For the second normalized Hamiltonian $\tilde{\mathcal{H}}$ (10) this means that the periodic orbits have detached from p_+. This situation clearly corresponds to a supercritical Hamiltonian Hopf bifurcation.

In the second case (Figs. 4c and d) the level curves of $\bar{\mathcal{H}}_0$ 'bend inwards', that is, when the level curve that passes through p becomes tangent to the line $w = \pi_2$, the rest of the level curve stays inside $V_{n,0}^0$. When $\lambda > 1$ (Fig. 4c) there are tangencies between the level curves and $V_{n,c}^*$ very close to p but they stop when $|c|$ becomes larger than some $c_0 > 0$. As λ decreases so does c_0 and the set of equilibria shrinks towards p. When $\lambda < 1$ (Fig. 4d) the level
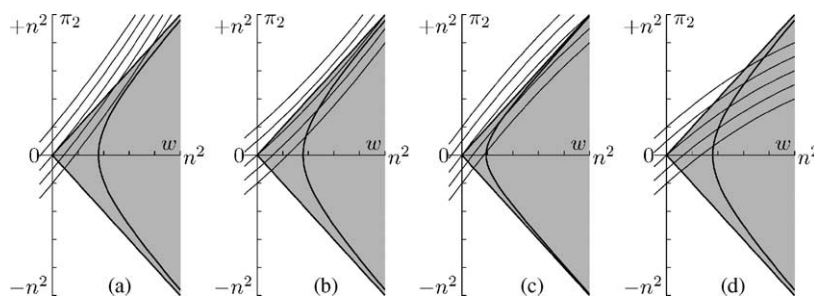

Fig. 4. Different types of Hamiltonian Hopf bifurcation, correspond to different relative arrangements of $V_{n,0}^0$ and the level curves of $\bar{\mathcal{H}}_0$. (a) and (b) The level curves of $\bar{\mathcal{H}}_0$ 'bend outwards' and the system goes through a supercritical Hamiltonian Hopf bifurcation. (c) and (d) The level curves of $\bar{\mathcal{H}}_0$ 'bend inwards' and the system goes through a subcritical Hamiltonian Hopf bifurcation.
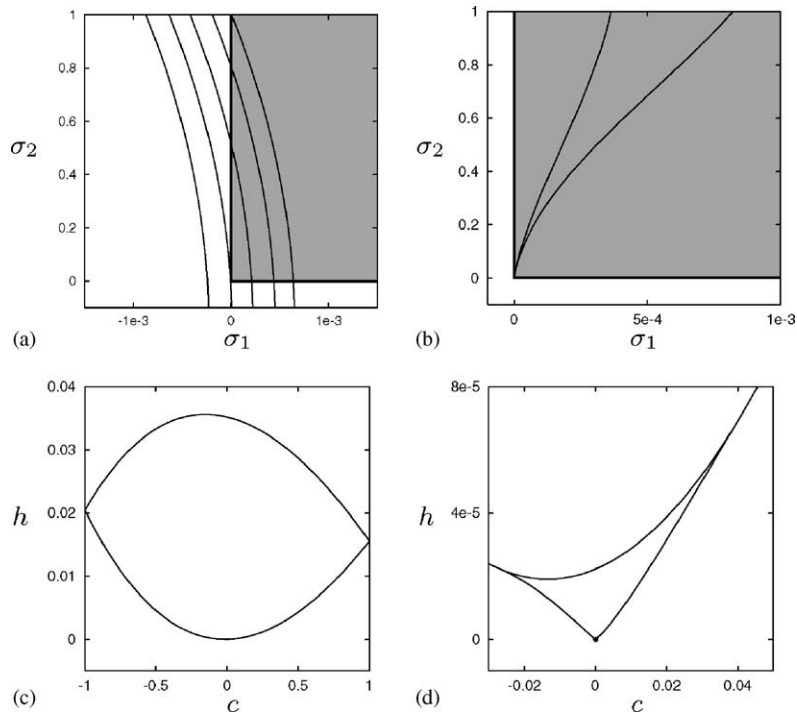
Fig. 5. Supercritical bifurcation. Here $a = a_1 + 10^{-4}$. (a) Level curves of $\bar{\mathcal{H}}_0$. (b) Family of critical points of $\bar{\mathcal{H}}_c$. In these two parts the coordinates are $\sigma_1 = (w - \pi_2)/2$ and $\sigma_2 = (w + \pi_2)/2$. The shaded region represents $V_{n,0}^0$. The horizontal axis $\sigma_1 = 0$ corresponds to the line $w = \pi_2$ of $V_{n,0}^*$. The vertical axis $w = -\pi_2$ corresponds to the line $w = -\pi_2$ of $V_{n,c}^*$. (c) The image of the energy–momentum map. (d) Blow up of a region around $(0, 0)$.

curves that pass near p enter $V_{n,0}^0$ in such a way that they intersect transversely all $V_{n,c}^*$ and therefore there are no critical points of $\bar{\mathcal{H}}_c$ near p. This situation clearly corresponds to the scenario of the subcritical bifurcation, where a family of periodic orbits shrinks towards the equilibrium point and then disappears.

In order to depict the Hamiltonian Hopf bifurcations on the fully reduced space and the image of the energy–momentum map $\mathcal{EM}$ we fix $n = 1$, $\epsilon = 1/10$ and find numerically the relative equilibria in the fully reduced phase space for values of a close to the bifurcation parameters $a_1(0.1) = 0.841102\ldots$ and $a_2(0.1) = 0.4744664\ldots$.

When a passes through $a_1(\delta)$ we have a supercritical Hamiltonian Hopf bifurcation that is depicted in Figs. 5a–d and 6a–d. In order to show better the family of relative equilibria we have used coordinates $\sigma_1 = (w - \pi_2)/2$ and $\sigma_2 = (w + \pi_2)/2$. In Figs. 5a and 6a we show the level curves of the Hamiltonian $\bar{\mathcal{H}}_0$ intersecting $V_{n,0}^0$. It is clear that they 'bend outwards' and according to the argument at the beginning of the section this corresponds to a supercritical Hamiltonian Hopf bifurcation in accordance with Theorem 1. We now check in more detail what happens as we cross the parameter value $a = a_1(0.1)$. For $a > a_1(0.1)$ the coefficient $A(a, 0.1)$ is positive and the point p_+ is elliptic–elliptic. In this case there is a family of relative equilibria emanating from p and parametrized by c. These are depicted in Fig. 5b, where for each c we have drawn the position of the corresponding relative equilibrium. These positions form two curves and each point on these curves corresponds to a relative equilibrium on a different fully reduced space $V_{n,c}^0$. The two branches correspond to different signs of c, so if we consider the intersection of some $V_{n,c}$ with the branch, it consists of only one point. This follows because one of the two points corresponds to $V_{n,c}$ and the other to $V_{n,-c}$. The two branches do not coincide, even though $V_{n,c}^0$ and $V_{n,-c}^0$ are identical, because the reduced Hamiltonian is not invariant with respect to the change $c \to -c$. For $a < a_1(0.1)$

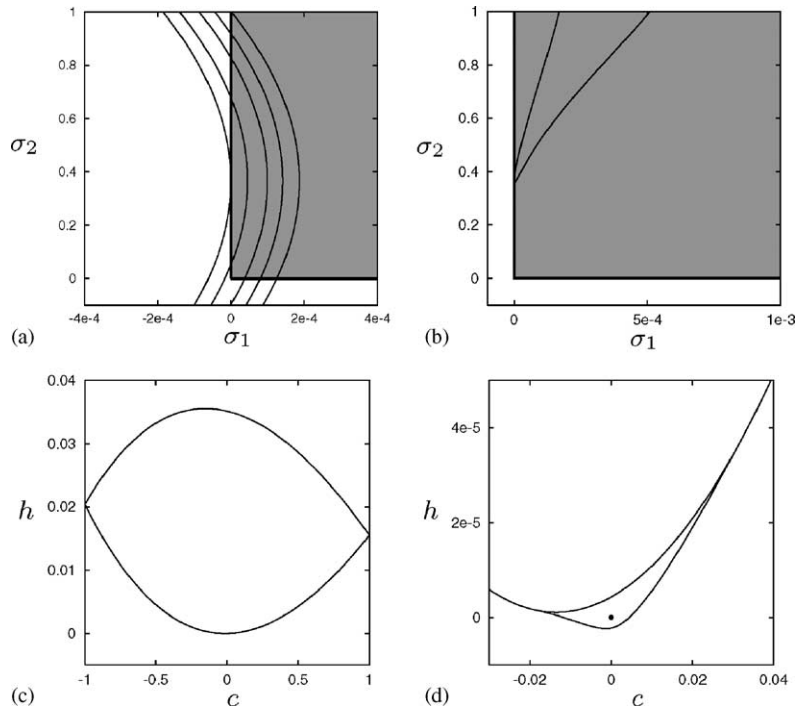Fig. 6. Supercritical bifurcation. Here $a = a_1 - 2 \times 10^{-4}$. (a) Level curves of $\bar{\mathcal{H}}_0$. (b) Family of critical points of $\bar{\mathcal{H}}_c$. (c) The image of the energy–momentum map. (d) Blow up of a region around $(0, 0)$.

the coefficient $A(a, 0.1)$ becomes negative and the point p_+ becomes complex hyperbolic. The family of relative equilibria detaches from p_+ and moves away. The situation is depicted in Fig. 6b where again the two branches correspond to the values of c and $-c$.

One can also see the Hamiltonian Hopf bifurcation in the image of the energy momentum map, $\mathcal{EM} : (\mathbf{S}^2 \times \mathbf{S}^2) \to \mathbf{R}^2 : z \mapsto (\tilde{\mathcal{H}}(z), \tilde{\mathcal{H}}_1(z))$. Specifically for $a > a_1$ we have drawn the image of the $\mathcal{EM}$ map in Fig. 5c and a blow up of a small region in Fig. 5d. We see there that at $(0, 0)$ we have a critical point that corresponds to the image of p_+ and this is connected to a family of relative equilibria. For $a < a_1$ (Fig. 6c and d) we see that the critical point p_+ has detached from the family of relative equilibria and is isolated. Therefore in this case we have monodromy that appears as a result of the supercritical Hamiltonian Hopf bifurcation.

In the case of the subcritical bifurcation the level set $\bar{\mathcal{H}}_0^{-1}(0, 0)$ becomes tangent to the line $w = -\pi_2$. In Fig. 7a we show the level curves of the Hamiltonian. It is clear that they 'bend inwards'. According to the argument above it corresponds to a subcritical Hamiltonian Hopf bifurcation in accordance with Theorem 1. We now check in more detail what happens as we cross the value $a = a_2(\delta)$. For $a > a_2(\delta)$, p_+ is complex hyperbolic and there are not any relative equilibria close to it. For $a < a_2$, the point p_+ becomes elliptic–elliptic and in the fully reduced space we have a family of critical points of $\bar{\mathcal{H}}_c$ emanating from p. The family is depicted in Fig. 7b. For $c = 0$ the family has two points O and O'. For $c = c_- < 0$ the family has the point O^- and for $c = c_+ > 0$ it has the point O^+. For each $c \in (c_-, 0)$ the family has two points on the curve $\mathrm{OO}^-\mathrm{O}'$, one on OO^- and one on $\mathrm{O}'\mathrm{O}^-$. For each $c \in (0, c_+)$ the family has two points on $\mathrm{OO}^+\mathrm{O}'$, one on the curve OO^+ and one on $\mathrm{O}'\mathrm{O}^+$.

In the image of $\mathcal{EM}$ we see a very small 'triangular' are (Fig. 7d) with $\mathcal{EM}(p_+)$ being at one of the vertices of the 'triangle'. Again, $\mathcal{EM}(p_+) = (0, 0)$ is connected to a family of critical points of $\mathcal{EM}$ which are equilibria of
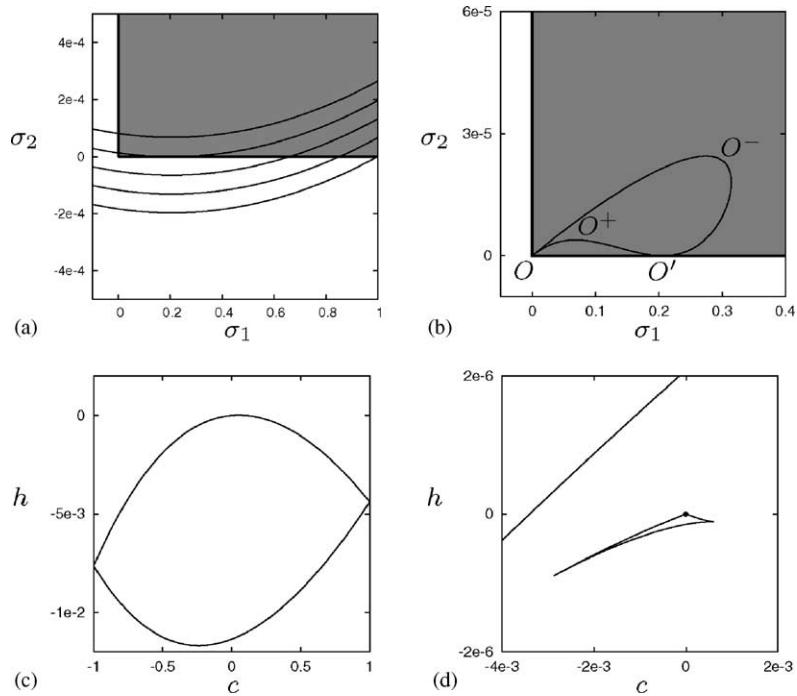
Fig. 7. Subcritical bifurcation. Here $a = a_2 - 25 \times 10^{-6}$. (a) Level curves of $\bar{\mathcal{H}}_0$. (b) Family of critical points of $\bar{\mathcal{H}}_c$. (c) The image of the energy–momentum map. (d) Blow up of a region of (c) around $(0, 0)$.

the reduced Hamiltonian. As a increases and approaches a_2 from below the 'triangular' area shrinks and exactly at $a = a_2$ it disappears leaving in its place an isolated critical point.

In this case we have monodromy both before and after the Hamiltonian Hopf bifurcation. When $a > a_2$ we have the classical type of monodromy around the isolated critical point. When $a < a_2$ we have *non-local monodromy* [12]. This means that if we consider a closed path Γ around the 'triangle' in Fig. 7d, the $\mathbf{T}^2$ bundle $\mathcal{EM}^{-1}(\Gamma)$ is not trivial. Since the passage from $a > a_2$ to $a < a_2$ is a smooth deformation the monodromy around the 'triangle' for $a < a_2$ must be the same as the monodromy around the critical point for $a > a_2$, i.e. it is given by the matrix

$$\begin{pmatrix} 1 & 2 \\ 0 & 1 \end{pmatrix}.$$

The last question is how does monodromy disappear as we lower the value of a and approach the Stark limit. The answer is that there exists another family of relative equilibria that is not related directly to the Hamiltonian Hopf bifurcations. The image of this family under $\mathcal{EM}$ is connected to the rest of the boundary of the image of $\mathcal{EM}$. At $a = a_j \simeq a_2 - 27 \times 10^{-6}$ this family and the family of relative equilibria related to the Hamiltonian Hopf bifurcation join. For $a < a_j$ there do not exist any other families of relative equilibria disconnected from the boundary of the image of $\mathcal{EM}$ and therefore the system can not have monodromy. For more details on these families see [29].

5. Conclusions

We have proved that the hydrogen atom in crossed fields goes through two Hamiltonian Hopf bifurcations when the relevant parameter of the system enters or leaves the interval of parameter values for which this system has

monodromy. We also uncovered the fine details of these bifurcations such as non-local monodromy. The proof is traditionally analytic along the lines in [23]. We also detailed a complementary geometric description based on the qualitative study of the level curves of the fully reduced Hamiltonian on the fully reduced space. Anticipated in [10], this description can by itself provide a complete proof of the occurrence of the Hamiltonian Hopf bifurcations and their characterization. A similar approach was developed in [30,31]. What we add to this is the use of the *fully* reduced system which allows to decrease the degree of the Hamiltonian from 4 to 2. Clearly, formalizing and developing this geometric analysis for its application to the concrete system goes beyond the scope of the more 'traditional' approach adopted initially in the present paper. Such geometric study should be deferred to a future work and will certainly constitute an important new contribution to the field.

The physical significance of these bifurcations is an equally important subject of future analysis. The relative equilibria that participate in these bifurcations are not 'closed orbits', i.e., trajectories of the electron that go to the nucleus [9,32–34]. So these bifurcations would not be observed 'directly' in Rydberg spectra, but they would certainly affect qualitatively the form of the wave functions.

In the integrable approximation these bifurcations are related to monodromy whose implication in the actual quantum system has been understood only partially [10]. The global role of these bifurcations in the original non-integrable system is in creating centers of strongly chaotic dynamics. Continuing certain aspects of the integrable approximation, namely sequences of bifurcations including the Hamiltonian Hopf bifurcation, into the chaotic region near the ionization threshold is therefore an important future direction of research.

Acknowledgements

Appendix A. Review of the Keplerian normalization

A.1. Kustaanheimo–Stiefel regularization

The Kustaanheimo–Stiefel regularization is a standard procedure for the regularization of the Kepler vector field. The first step is a time rescaling which is also used in Moser regularization.

Specifically, we fix an energy level $E < 0$ (since we are only interested in bounded motions), rescale $(Q, P) \rightarrow (C^{-1}Q, CP)$ and introduce the new time scale $\mathrm{d}t \rightarrow C^2 \, \mathrm{d}t/|Q|$. The result is

$$1 = \frac{1}{2}\left(P^2 - \frac{2E}{C^2}\right)|Q| + \frac{F}{C^3}Q_2|Q| + \frac{G}{2C^2}(Q_2 P_3 - Q_3 P_2)|Q| + \frac{G^2}{8C^4}(Q_2^2 + Q_3^2)|Q|, \tag{A.1}$$

where

$$H_0 = \frac{1}{2}\left(P^2 - \frac{2E}{C^2}\right)|Q| \tag{A.2}$$

is the unperturbed Hamiltonian.

The Kustaanheimo–Stiefel regularization is defined by the transformation

$$\mathrm{KS} : T_0\mathbf{R}^4 \rightarrow T_0\mathbf{R}^3 : (q, p) \mapsto \left(M(q)q, \frac{1}{q^2}M(q)p\right) = (Q, 0, P, 0), \tag{A.3}$$

where $M(q)$ is the matrix

$$M(q) = \begin{pmatrix} q_1 & -q_2 & -q_3 & q_4 \\ q_2 & q_1 & -q_4 & -q_3 \\ q_3 & q_4 & q_1 & q_2 \\ q_4 & -q_3 & q_2 & -q_1 \end{pmatrix}. \tag{A.4}$$

Notice that

$$\zeta = \tfrac{1}{2}(q_1 p_4 - q_2 p_3 + q_3 p_2 - q_4 p_1) = 0, \tag{A.5}$$

and that ζ generates an $\mathbf{S}^1$ action on $T_0 \mathbf{R}^4$ called the KS symmetry.

Any function defined on $T_0 \mathbf{R}^4$ through the KS transformation Poisson commutes with ζ. Therefore we can treat ζ as a constant of motion identically equal to 0.

The KS transformed Hamiltonian after the scaling $(q, p) \to (q/\sqrt{\omega}, p\sqrt{\omega})$ and changing the time by $t \to \omega t$ becomes

$$H = \tfrac{1}{2}(p^2 + q^2) + \tfrac{1}{3} f(q_1 q_2 - q_3 q_4)q^2 + \tfrac{1}{2} g(q_2 p_3 - q_3 p_2)q^2 + \tfrac{1}{8} g^2(q_1^2 + q_4^2)(q_2^2 + q_3^2)q^2, \tag{A.6}$$

where

$$\omega^2 = -\frac{2E}{C^2}, \qquad f = \frac{6F}{C^3 \omega^3} = \epsilon b, \qquad g = \frac{2G}{C^2 \omega^2} = \epsilon a, \qquad a^2 + b^2 = 1. \tag{A.7}$$

A.2. First normalization

We normalize the Hamiltonian (A.6) with respect to the unperturbed part $H_0 = (1/2)(q^2 + p^2)$, which is the Hamiltonian of a 1:1:1:1 resonant harmonic oscillator. The result of the normalization and truncation is the Hamiltonian

$$\tilde{H} = \tilde{H}_2 + \epsilon \tilde{H}_4 + \epsilon^2 \tilde{H}_6 + \epsilon^3 \tilde{H}_8 + \epsilon^4 \tilde{H}_{10}, \tag{A.8}$$

where each term $\tilde{H}_j$ is a homogeneous polynomial of degree j in (q, p). Expressions for $\tilde{H}$ can be easily obtained from the expressions of the reduced Hamiltonian $\hat{H}$ given later in Table 2.

A.3. First reduction

The algebra $\mathbf{R}[q, p]^{\mathbf{T}^2}$ of the polynomials that are invariant under the $\mathbf{T}^2$ action generated by H_0 and ζ is generated by the invariant polynomials

$$\begin{aligned}
K_1 &= \tfrac{1}{4}(p_2^2 + q_2^2 + p_3^2 + q_3^2 - p_1^2 - q_1^2 - p_4^2 - q_4^2), & K_2 &= \tfrac{1}{2}(p_3 p_4 - q_1 q_2 - p_1 p_2 + q_3 q_4), \\
K_3 &= -\tfrac{1}{2}(q_1 q_3 + q_2 q_4 + p_1 p_3 + p_2 p_4), & L_1 &= \tfrac{1}{2}(q_2 p_3 - q_3 p_2 + q_1 p_4 - q_4 p_1), \\
L_2 &= \tfrac{1}{2}(q_2 p_4 + q_3 p_1 - q_1 p_3 - q_4 p_2), & L_3 &= \tfrac{1}{2}(q_1 p_2 + q_3 p_4 - q_2 p_1 - q_4 p_3), \\
n &= \tfrac{1}{4}(p_2^2 + q_2^2 + p_3^2 + q_3^2 + p_1^2 + q_1^2 + p_2^2 + q_2^2), & \zeta &= \tfrac{1}{2}(q_1 p_4 - q_2 p_3 + q_3 p_2 - q_4 p_1).
\end{aligned} \tag{A.9}$$

The vectors $K = (K_1, K_2, K_3)$ and $L = (L_1, L_2, L_3)$ are the KS transformed eccentricity vector and angular momentum vector, respectively. The invariant polynomials satisfy the relations

$$K^2 + L^2 = n^2 + \zeta^2, \quad KL = -n\zeta. \tag{A.10}$$

Table A.1
Coefficients of the terms of the first normal form $\tilde{H}$

Coefficients of terms of $72\tilde{H}_6$	
n^2	$-17b^2$
L_3^2	$9a^2$
L_2^2	$9a^2 + 9b^2$
K_3^2	$45a^2$
$K_2 L_1$	$84ab$
K_2^2	$45a^2 - 51b^2$
$K_1 L_2$	$-12ab$
Coefficients of terms of $288\tilde{H}_8$	
$n^2 L_1$	$337ab^2$
$L_1 L_3^2$	$-54a^3 - 102ab^2$
$L_1 L_2^2$	$-54a^3 - 192ab^2$
L_1^3	$-72a^3 - 102ab^2$
$K_3 L_2 L_3$	$-144a^2 b$
$K_3^2 L_1$	$-270a^3 - 108ab^2$
$n^2 K_2$	$156a^2 b - 250b^3$
$K_2 L_3^2$	$60a^2 b$
$K_2 L_2^2$	$-84a^2 b + 86b^3$
$K_2 L_1^2$	$-246a^2 b$
$K_2 K_3^2$	$330a^2 b$
$K_2^2 L_1$	$-270a^3 + 510ab^2$
K_2^3	$330a^2 b - 250b^3$
$K_1 K_3 L_3$	$108ab^2$
Coefficients of terms of $13\,824\tilde{H}_{10}$	
n^4	$1504a^2 b^2 - 3563b^4$
$n^2 L_3^2$	$36a^4 + 1086a^2 b^2$
L_3^4	$-351a^4 - 240a^2 b^2$
$n^2 L_2^2$	$36a^4 - 1110a^2 b^2 + 2970b^4$
$L_2^2 L_3^2$	$-702a^4 - 278a^2 b^2$
L_2^4	$-351a^4 - 38a^2 b^2 - 303b^4$
$n^2 L_1^2$	$10\,224a^4 - 66\,192a^2 b^2$
$L_1^2 L_3^2$	$-9072a^4 + 46\,736a^2 b^2$
$L_1^2 L_2^2$	$-9072a^4 + 53\,712a^2 b^2$
L_1^4	$-6768a^4 + 46\,976a^2 b^2$
$K_3 L_1 L_2 L_3$	$12\,312a^3 b + 120ab^3$
$n^2 K_3^2$	$-4716a^4 + 9462a^2 b^2$
$K_3^2 L_3^2$	$-12\,690a^4 + 48\,080a^2 b^2$
$K_3^2 L_2^2$	$-2358a^4 - 2334a^2 b^2$
$K_3^2 L_1^2$	$48\,080a^2 b^2$
K_3^4	$-5895a^4$
$n^2 K_2 L_1$	$-27\,768a^3 b + 74\,320ab^3$
$K_2 L_1 L_3^2$	$-5976a^3 b - 10\,056ab^3$

Table A.1 (*Continued*)

$K_2 L_1 L_2^2$	$6336 a^3 b - 27\,312 ab^3$
$K_2 L_1^3$	$2784 a^3 b - 10\,056 ab^3$
$K_2 K_3 L_2 L_3$	$-20\,664 a^4 + 70\,888 a^2 b^2$
$K_2 K_3^2 L_1$	$-47\,520 a^3 b - 11\,232 ab^3$
$n^2 K_2^2$	$-4716 a^4 + 38\,978 a^2 b^2 - 35\,630 b^4$
$K_2^2 L_3^2$	$-2358 a^4 + 5266 a^2 b^2$
$K_2^2 L_2^2$	$-12\,690 a^4 + 25\,740 a^2 b^2 + 8910 b^4$
$K_2^2 K_3^2$	$-11\,790 a^4 + 31\,290 a^2 b^2$
$K_2^3 L_1$	$-47\,520 a^3 b + 48\,000 ab^3$
K_2^4	$-5895 a^4 + 31\,290 a^2 b^2 - 17\,815 b^4$
$n^2 K_1 L_2$	$-336 a^3 b - 4352 ab^3$
$K_1 L_2 L_3^2$	$768 a^3 b - 120 ab^3$
$K_1 L_2^3$	$768 a^3 b + 744 ab^3$
$K_1 K_3^2 L_2$	$3720 a^3 b$
$K_1 K_2 K_3 L_3$	$-3720 a^3 b + 11\,232 ab^3$

The space of $\mathbf{T}^2$ orbits on $H_0^{-1}(2n) \cap \zeta^{-1}(0)$ is defined by

$$K^2 + L^2 = n^2, \qquad KL = 0, \tag{A.11}$$

or equivalently

$$(K + L)^2 = n^2, \qquad (K - L)^2 = n^2. \tag{A.12}$$

Therefore the orbit space is $\mathbf{S}^2 \times \mathbf{S}^2$. The Poisson structure on the reduced space is

$$\{L_i, L_j\} = \sum_k \varepsilon_{ijk} L_k, \qquad \{K_i, K_j\} = \sum_k \varepsilon_{ijk} L_k, \qquad \{L_i, K_j\} = \sum_k \varepsilon_{ijk} K_k. \tag{A.13}$$

After computing the normal form we perform $\mathbf{T}^2$ reduction by expressing the normalized Hamiltonian (A.8) in terms of the polynomials (A.9). The result is

$$\hat{H} = \hat{H}_2 + \epsilon \hat{H}_4 + \epsilon^2 \hat{H}_6 + \epsilon^3 \hat{H}_8 + \epsilon^4 \hat{H}_{10}. \tag{A.14}$$

After setting $\zeta = 0$ the first terms of $\hat{H}$ are

$$\hat{H}_2 = 2n, \tag{A.15}$$

$$\hat{H}_4 = n(aL_1 - bK_2). \tag{A.16}$$

The coefficients for the other terms are presented in Table 2. Next we subtract the constant term $\hat{H}_2 = 2n$ and then divide $\hat{H}$ by $n\epsilon$.

In the resulting rescaled Hamiltonian, called the first reduced Hamiltonian, we make the successive linear changes of variables

$$\begin{aligned} T_1 &= aL_1 - bK_2, & T_2 &= aL_2 + bK_1, & T_3 &= L_3, \\ V_1 &= aK_1 - bL_2, & V_2 &= aK_2 + bL_1, & V_3 &= K_3, \end{aligned} \tag{A.17}$$

and

$$x_1 = \tfrac{1}{2}(T_1 + V_1), \qquad x_2 = \tfrac{1}{2}(T_2 + V_2), \qquad x_3 = \tfrac{1}{2}(T_3 + V_3),$$
$$y_1 = \tfrac{1}{2}(T_1 - V_1), \qquad y_2 = \tfrac{1}{2}(T_2 - V_2), \qquad y_3 = \tfrac{1}{2}(T_3 - V_3). \tag{A.18}$$

The variables x, y satisfy

$$x_1^2 + x_2^2 + x_3^2 = \tfrac{1}{4}n^2, \qquad y_1^2 + y_2^2 + y_3^2 = \tfrac{1}{4}n^2. \tag{A.19}$$

They span the algebra so(3) × so(3) = so(4). The Poisson structure is given by (3).

The lowest order non-trivial term of the first reduced Hamiltonian becomes

$$\mathcal{H}_1 = \hat{H}_4 = x_1 + y_1. \tag{A.20}$$

We define $\mathcal{H}_j = \hat{H}_{2j+2}$. Notice that $\mathcal{H}_j$ is a homogeneous polynomial of degree j in (x, y, n). The first reduced Hamiltonian can be written in terms of (x, y, n) variables as

$$\mathcal{H} = \mathcal{H}_1 + \epsilon \mathcal{H}_2 + \epsilon^2 \mathcal{H}_3 + \epsilon^3 \mathcal{H}_4, \tag{A.21}$$

where $\mathcal{H}_1 = x_1 + y_1$, and the rest of the terms can be computed straightforwardly from Table 2 using (A.17) and (A.18).

Appendix B. Full reduction and reconstruction

B.1. Second reduction

We recall here that Keplerian normalization creates an approximate $\mathbf{S}^1$ axial symmetry Φ (6) on $\mathbf{S}^2 \times \mathbf{S}^2$. The algebra $\mathbf{R}[x, y]^\Phi$ of Φ-invariant polynomials in the variables (x, y) is generated by

$$\pi_1 = x_1 - y_1, \qquad \pi_2 = 4(x_2 y_2 + x_3 y_3), \qquad \pi_3 = 4(x_3 y_2 - x_2 y_3),$$
$$\pi_4 = x_1 + y_1, \qquad \pi_5 = 4(x_2^2 + x_3^2), \qquad \pi_6 = 4(y_2^2 + y_3^2). \tag{B.1}$$

These invariants satisfy

$$\pi_2^2 + \pi_3^2 = \pi_5 \pi_6, \quad \pi_5 \geq 0, \ \ \pi_6 \geq 0. \tag{B.2}$$

From (A.19) we have

$$\pi_5 = n^2 - (\pi_1 + \pi_4)^2, \qquad \pi_6 = n^2 - (\pi_1 - \pi_4)^2. \tag{B.3}$$

Since $\pi_4 = c$, the second reduced phase space $M_{n,c}$ is the semi-algebraic variety defined by

$$\pi_2^2 + \pi_3^2 = (n^2 - (\pi_1 + c)^2)(n^2 - (\pi_1 - c)^2), \quad |\pi_1| \leq n - |c|. \tag{B.4}$$

Notice that in the space $\mathbf{R}^3$ with coordinates (π_1, π_2, π_3) the spaces $M_{n,c}$ and $M_{n,-c}$ have the same representation. The Poisson structure on $M_{n,c}$ is

$$\{\pi_1, \pi_2\} = 2\pi_3, \qquad \{\pi_1, \pi_3\} = -2\pi_2, \qquad \{\pi_2, \pi_3\} = 4\pi_1(n^2 + c^2 - \pi_1^2). \tag{B.5}$$

Expressing $\tilde{\mathcal{H}}$ (10) in terms of π_1, π_2, π_3 and $\pi_4 = c$ gives the second reduced Hamiltonian

$$\hat{\mathcal{H}} = \hat{\mathcal{H}}_1 + \epsilon \hat{\mathcal{H}}_2 + \epsilon^2 \hat{\mathcal{H}}_3 + \epsilon^3 \hat{\mathcal{H}}_4, \tag{B.6}$$

Table B.1
Coefficients of the terms of the second reduced Hamiltonian $\hat{\mathcal{H}}$

Coefficients of terms of $72\hat{\mathcal{H}}_2$

π_2	$-18a^2$
π_1^2	$9 - 18a^2 - 18a^4$
c^2	$-51 + 42a^2 - 18a^4$
n^2	$-17 + 38a^2 + 6a^4$

Coefficients of terms of $288\hat{\mathcal{H}}_3$

$\pi_2 c$	$136a^2 - 16a^4 - 12a^6$
$\pi_1^2 c$	$-86 + 168a^2 - 10a^4 + 192a^6 - 102a^8$
c^3	$250 - 304a^2 + 122a^4 + 56a^6 - 34a^8$
$n^2 c$	$250 - 576a^2 + 178a^4 - 32a^6 + 18a^8$

Coefficients of terms of $13\,824\hat{\mathcal{H}}_4$

π_2^2	$-1020a^4 + 48a^6 + 144a^8 - 144a^{10}$
π_1^4	$-303 + 1252a^2 - 304a^4 + 996a^6 - 3792a^8 + 1500a^{10} - 1500a^{12}$
$\pi_2 n^2$	$-4908a^2 + 8104a^4 + 2004a^6 + 56a^8 - 108a^{10}$
$\pi_1^2 \pi_2$	$1140a^2 - 2104a^4 - 1412a^6 + 264a^8 - 660a^{10}$
$\pi_1^2 n^2$	$2970 - 11\,048a^2 + 8528a^4 - 1064a^6 + 7640a^8 - 1416a^{10} + 1032a^{12}$
$\pi_1^2 c^2$	$8910 - 19\,896a^2 + 8016a^4 - 9144a^6 - 16\,608a^8 + 27\,624a^{10} - 9000a^{12}$
$\pi_2 c^2$	$-13\,092a^2 + 6136a^4 - 996a^6 + 1256a^8 - 612a^{10}$
$n^2 c^2$	$-35\,630 + 91\,624a^2 - 54\,800a^4 + 6888a^6 + 5784a^8 - 2568a^{10} + 1032a^{12}$
c^4	$-17\,815 + 28\,628a^2 - 16\,320a^4 - 1292a^6 + 240a^8 + 3676a^{10} - 1500a^{12}$
n^4	$-3563 + 13\,252a^2 - 11\,472a^4 - 860a^6 - 1848a^8 + 44a^{10} - 44a^{12}$

where

$$\hat{\mathcal{H}}_1 = \pi_4 = c. \tag{B.7}$$

The coefficients of the terms $\hat{\mathcal{H}}_2$, $\hat{\mathcal{H}}_3$ and $\hat{\mathcal{H}}_4$ are given in Table 3.

B.2. Discrete symmetries and full reduction

We can take into account the discrete symmetries of the original system in order to simplify our analysis. The original Hamiltonian (1) is invariant with respect to a group of discrete symmetries that consists of the transformations

$$
\begin{aligned}
g_1 &: (Q_1, Q_2, Q_3, P_1, P_2, P_3) \mapsto (-Q_1, Q_2, -Q_3, P_1, -P_2, P_3), \\
g_2 &: (Q_1, Q_2, Q_3, P_1, P_2, P_3) \mapsto (-Q_1, Q_2, Q_3, -P_1, P_2, P_3), \\
g_3 &: (Q_1, Q_2, Q_3, P_1, P_2, P_3) \mapsto (Q_1, Q_2, -Q_3, -P_1, -P_2, P_3).
\end{aligned}
\tag{B.8}
$$

Each g_i generates a $\mathbf{Z}_2$ subgroup of the full symmetry group, which is isomorphic to $\mathbf{Z}_2 \times \mathbf{Z}_2$.

The induced transformations on the second reduced space $M_{n,c}$ are

$$
\begin{aligned}
g_1 &: (\pi_1, \pi_2, \pi_3) \mapsto (-\pi_1, \pi_2, \pi_3), \qquad g_2 : (\pi_1, \pi_2, \pi_3) \mapsto (-\pi_1, \pi_2, -\pi_3), \\
g_3 &: (\pi_1, \pi_2, \pi_3) \mapsto (\pi_1, \pi_2, -\pi_3).
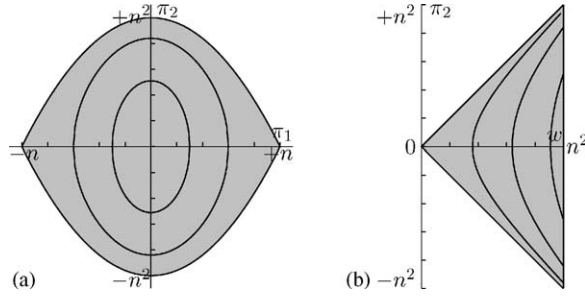\end{aligned}
\tag{B.9}
$$

Fig. 8. (a) Reduced phase spaces $M_{n,c}^0$. (b) Fully reduced phase spaces $V_{n,c}^0$.

The orbit space $M_{n,c}^0$ of the $\mathbf{Z}_2$ action generated by g_3 is the image of $M_{n,c}$ under the map $\mathbf{R}^3 \to \mathbf{R}^2$: $(\pi_1, \pi_2, \pi_3) \mapsto (\pi_1, \pi_2)$ (Fig. 8a). $\partial M_{n,c}^0$ is the boundary of $M_{n,c}^0$ or equivalently as the intersection of $M_{n,c}$ with the plane $\{\pi_3 = 0\}$.

The orbit space $V_{n,c}$ of the $\mathbf{Z}_2$ action on $M_{n,c}$ generated by g_1 is the image of $M_{n,c}$ under the map $\mathbf{R}^3 \to \mathbf{R}^3$: $(\pi_1, \pi_2, \pi_3) \mapsto (w, \pi_2, \pi_3)$, where $w = n^2 - \pi_1^2$. The *fully* reduced space $V_{n,c}^0$ can be defined equivalently as

- The orbit space of the $\mathbf{Z}_2$ action on $V_{n,c}$ generated by g_3. It is the image of $V_{n,c}$ under the map $\mathbf{R}^3 \to \mathbf{R}^2$: $(w, \pi_2, \pi_3) \mapsto (w, \pi_2)$.
- The orbit space of the $\mathbf{Z}_2$ action on $M_{n,c}^0$ generated by g_1. It is the image of $M_{n,c}^0$ under the map $\mathbf{R}^2 \to \mathbf{R}^2$: $(\pi_1, \pi_2) \mapsto (w, \pi_2)$.
- The orbit space of the full $\mathbf{Z}_2 \times \mathbf{Z}_2$ action on $M_{n,c}$. It is the image of $M_{n,c}$ under the map $\mathbf{R}^3 \to \mathbf{R}^2$: $(\pi_1, \pi_2, \pi_3) \mapsto (w, \pi_2)$.

Finally, $V_{n,c}^*$ is the boundary of $V_{n,c}^0$ less the line segment $\{(n^2, \pi_2) : -c \leq \pi_2 \leq c\}$. Points on $V_{n,c}^*$ satisfy the equation

$$\pi_2^2 = (w + c^2)^2 - (2nc)^2. \tag{B.10}$$

The fully reduced Hamiltonian $\bar{\mathcal{H}}_c$ on $V_{n,c}$ is obtained from $\hat{\mathcal{H}}$ (B.6) (see also Table 3) by the substitution $\pi_1^2 = n^2 - w$.

At this point let us complete the argument used in Section 1 to explain why we need to compute the four-jet of $\tilde{\mathcal{H}}$ in order to lift the degeneracy of the Hamiltonian Hopf bifurcation. The discrete symmetry group $\mathbf{Z}_2 \times \mathbf{Z}_2$ imposes certain restrictions on the types of terms that can appear in the fully reduced Hamiltonian $\bar{\mathcal{H}}_c$. The allowed terms appear in Table 4, where $\bar{\mathcal{H}}_{c,j}$ is the part of $\bar{\mathcal{H}}_c$ that comes from $\tilde{\mathcal{H}}_j$, i.e. the part of $\tilde{\mathcal{H}}$ of degree j. It is clear from the table that if we consider $\bar{\mathcal{H}}_c$ only up to $\bar{\mathcal{H}}_{c,2}$ as it was done in [10], or even up to $\bar{\mathcal{H}}_{c,3}$, its level curves will appear in the plane (w, π_2) as straight lines. In order to correct this we need to go to $\bar{\mathcal{H}}_{c,4}$, i.e. up to fourth degree terms in $\tilde{\mathcal{H}}$.

Table B.2
Terms compatible with $\mathbf{Z}_2 \times \mathbf{Z}_2$ symmetry

Part of $\bar{\mathcal{H}}_c$	Allowed terms
$\bar{\mathcal{H}}_{c,1}$	c
$\bar{\mathcal{H}}_{c,2}$	w, π_2, c^2, n^2
$\bar{\mathcal{H}}_{c,3}$	$wc, \pi_2 c, c^3, n^2 c$
$\bar{\mathcal{H}}_{c,4}$	$w\pi_2, \pi_2^2, \pi_2 c^2, \pi_2 n^2, w^2, wc^2, wn^2, c^4, n^2 c^2, n^4$

B.3. Reconstruction

Since $V_{n,c}^0$ is the orbit space of $M_{n,c}^0$ with respect to the $\mathbf{Z}_2$ symmetry generated by g_1 each point of $V_{n,c}^0 \setminus \{w = n^2\}$ lifts to two points in $M_{n,c}^0$; while each point on the line $\{w = n^2\}$ lifts to one point.

$M_{n,c}^0$ is the orbit space of $M_{n,c}$ with respect to the $\mathbf{Z}_2$ symmetry generated by g_3. Therefore, each point in the interior of $M_{n,c}^0$ lifts to two points in $M_{n,c}$ with opposite sign of π_3; while the points on $\partial M_{n,c}^0$ lift to one point.

Each point of $M_{n,c}$ lifts to an $\mathbf{S}^1$ orbit (a topological circle) on $\mathbf{S}^2 \times \mathbf{S}^2$. The only exceptions are the singular points of $M_{n,0}$ which lift to only one point on $\mathbf{S}^2 \times \mathbf{S}^2$, and the single points $M_{n,\pm n}$, which lift to two single points. Specifically, the singular point of $M_{n,0}$ with coordinates $(\pi_1, \pi_2, \pi_3) = (n, 0, 0)$ lifts to the point $p_+ = n/2(1, 0, 0, -1, 0, 0)$ while the point $(-n, 0, 0)$ lifts to the point $p_- = n/2(-1, 0, 0, 1, 0, 0)$. Each space $M_{n,\pm n}$ consists of a single point with coordinates $(\pi_1, \pi_2, \pi_3) = (0, 0, 0)$. These lift to the points $z_\pm$ on $\mathbf{S}^2 \times \mathbf{S}^2$ with coordinates $z_\pm = n/2(\pm 1, 0, 0, \pm 1, 0, 0)$. The points $p_\pm$ and $z_\pm$ are fixed points of the $\mathbf{S}^1$ action Φ (6) on $\mathbf{S}^2 \times \mathbf{S}^2$ and therefore are equilibria of any Φ invariant Hamiltonian on $\mathbf{S}^2 \times \mathbf{S}^2$.

References

[1] M. Kuwata, A. Harada, H. Hasegawa, Derivation and quantisation of Solov'ev's constant for the diamagnetic Kepler motion, J. Phys. A 23 (14) (1990) 3227–3244.
[2] D. Farrelly, K. Krantzman, Dynamical symmetry of the quadratic Zeeman effect in hydrogen: semiclassical quantization, Phys. Rev. A 43 (1991) 1666–1668.
[3] K.D. Krantzman, J.A. Milligan, D. Farrelly, Semiclassical mechanics of the quadratic Zeeman effect, Phys. Rev. A 45 (1992) 3093–3103.
[4] D. Farrelly, J.A. Milligan, Action-angle variables for the diamagnetic Kepler problem, Phys. Rev. A 45 (1992) 8277–8279.
[5] D. Farrelly, T. Uzer, P.E. Raines, J.P. Skelton, J.A. Milligan, Electronic structure of Rydberg atoms in parallel electric and magnetic fields, Phys. Rev. A 45 (1992) 4738–4751.
[6] D.A. Sadovskií, B.I. Zhilinskií, L. Michel, Collapse of the Zeeman structure of the hydrogen atom in an external electric field, Phys. Rev. A 53 (1996) 4064–4067.
[7] D.A. Sadovskií, B.I. Zhilinskií, Tuning the hydrogen atom in crossed fields between the Zeeman and Stark limits, Phys. Rev. A 57 (1998) 2867–2884.
[8] D.M. Wang, J.B. Delos, Organization and bifurcation of planar closed orbits of an atomic electron in crossed fields, Phys. Rev. A 63 (2001) 43409–43422.
[9] T. Bartsch, J. Main, G. Wunner, Closed orbits and their bifurcations in the crossed-field hydrogen atom, Phys. Rev. A 67 (2003) 063410.
[10] R.H. Cushman, D.A. Sadovskií, Monodromy in the hydrogen atom in crossed fields, Physica D 142 (2000) 166–196.
[11] R.H. Cushman, D.A. Sadovskií, Monodromy perturbed Kepler systems: hydrogen atom in crossed fields, Europhys. Lett. 47 (1999) 1–7.
[12] H. Waalkens, A. Junge, H.R. Dullin, Quantum monodromy in the two-centre problem, J. Phys. A 36 (2003) L307–L314.
[13] P. Kustaanheimo, E. Stiefel, Perturbation theory of Kepler motion based on spinor regularization, J. Reine Angew. Math. 219 (1965) 204–219.
[14] J.C. van der Meer, R.H. Cushman, Orbiting dust under radiation pressure, in: H.D. Doebner, J.D. Henning (Eds.), Proceedings of the XV International Conference on Differential Geometric Methods in Theoretical Physics, World Scientific, Singapore, 1987, pp. 403–414.
[15] R.H. Cushman, A survey of normalization techniques applied to perturbed Keplerian systems, in: K. Jones et al. (Ed.), Dynamics Reported, vol. 1 of new series, Springer-Verlag, New York, 1991, pp. 54–112.
[16] J. von Milczewski, T. Uzer, Chaos and order in crossed fields, Phys. Rev. E 55 (1997) 6540–6551.
[17] J. von Milczewski, D. Farrelly, T. Uzer, $1/r$ dynamics in external fields: 2D or 3D, Phys. Rev. Lett. 78 (1997) 2349–2352.
[18] J. von Milczewski, D. Farrelly, T. Uzer, Role of the atomic Coulomb center in ionization and periodic orbit selection, Phys. Rev. A 56 (1997) 657–670.
[19] W. Gröbner, Die Lie–Reihen und ihre Anwendungen, Deutscher Verlag der Wissenschaftern, Berlin, 1960.
[20] A. Deprit, Canonical transformations depending on a small parameter, Cel. Mech. 1 (1969) 12–30.
[21] J.J. Duistermaat, On global action-angle coordinates, Commun. Pure Appl. Math. 33 (1980) 687–706.
[22] R.H. Cushman, J.J. Duistermaat, Non-Hamiltonian monodromy, J. Diff. Eqs. 172 (2001) 42–58.
[23] J.C. van der Meer, The Hamiltonian Hopf Bifurcation, vol. 1160 of Lecture Notes in Mathematics, Springer, New York, 1985.
[24] A. Weinstein, Normal modes for nonlinear Hamiltonian systems, Invent. Math. 20 (1973) 47–57.
[25] J.J. Duistermaat, The monodromy in the Hamiltonian Hopf bifurcation, Z. Angew. Math. Phys. 49 (1998) 156–161.
[26] N.T. Zung, A note on focus-focus singularities, Diff. Geom. Appl. 7 (1997) 123–130.
[27] L. Michel, Points critiques des fonctions invariantes sur une G-varieté, C.R. Acad. Sci. Paris 272 (1971) 433–436.

[28] R.H. Cushman, L. Bates, Global Aspects of Classical Integrable Systems, Birkhauser, Basel, 1997.

[29] K. Efstathiou, D.A. Sadovskií, Monodromy in the hydrogen atom in crossed fields as a result of Hamiltonian Hopf bifurcation, in preparation.

[30] H. Hanßmann, J.C. van der Meer, On the Hamiltonian Hopf bifurcations in the 3D Hénon–Heiles family, J. Dyn. Diff. Eqs. 14 (2002) 657–695.

[31] H. Hanßmann, J.C. van der Meer, On non-degenerate Hamiltonian Hopf bifurcations in 3DOF systems, Preprint.

[32] M. Du, J. Delos, Effect of closed classical orbits on quantum spectra: ionization of atoms in a magnetic field. I. Physical picture and calculations, Phys. Rev. A 38 (1988) 1896–1912.

[33] M. Du, J. Delos, Effect of closed classical orbits on quantum spectra: ionization of atoms in a magnetic field. II. Derivation of formulas, Phys. Rev. A 38 (1988) 1913–1930.

[34] J. Gao, J. Delos, Quantum manifestations of bifurcations of closed orbits in the photoabsorption spectra of atoms in electric fields, Phys. Rev. A 56 (1997) 356–364.